Nat. Hazards Earth Syst. Sci. Discuss., 2, 7027–7059, 2014
www.nat-hazards-earth-syst-sci-discuss.net/2/7027/2014/
doi:10.5194/nhessd-2-7027-2014

Natural Hazards and Earth System Sciences
Open Access
Discussions

Hydrologic sensitivity of flood runoff and inundation: 2011 Thailand floods in the Chao Phraya River basin

T. Sayama[1], **Y. Tatebe**[1,*], **Y. Iwami**[1], **and S. Tanaka**[1,**]

[1]International Centre for Water Hazard and Risk Management, Public Works Research Institute, Tsukuba, Japan
[*]now at: CTI Engineering, Co. Ltd., Tokyo, Japan
[**]now at: Disaster Prevention Research Institute, Kyoto University, Uji, Japan

Received: 29 October 2014 – Accepted: 1 November 2014 – Published: 19 November 2014

Correspondence to: T. Sayama (t-sayama@pwri.go.jp)

Published by Copernicus Publications on behalf of the European Geosciences Union.

Abstract

Thailand floods in 2011 caused an unprecedented economic damage in the Chao Phraya River basin. To diagnose the flood hazard characteristics, this study analyzes the hydrologic sensitivity of flood runoff and inundation to rainfall. The motivation is to address why the seemingly insignificant monsoon rainfall, or 1.2 times more rainfall than past large floods including the ones in 1995 and 2006, resulted in such a devastating flooding. To quantify the hydrologic sensitivity, this study simulated a long-term rainfall-runoff and inundation for the entire river basin (160 000 km^2). The simulation suggested that the flood inundation volume in 2011 was 1.6 times more than past flood events. Furthermore the elasticity index suggested that 1 % increase in rainfall causes 2.3 % increase in runoff and 4.2 % increase in flood inundation. This study highlights the importance of sensitivity quantification for better understanding of flood hazard characteristics; and the presented approach is effective for the analysis at large river basins.

1 Introduction

The 2011 large-scale floods over the Chao Phraya River basin resulted in the worst economic flood damage to Thailand (The World Bank, 2012). The flooding appeared to be induced mainly by rainfall from five typhoons and tropical depressions between May and October. The total rainfall in the six months during the monsoon season was approximately 1400 mm, while previous large-scale floods were caused by a total rainfall of approximately 1200 mm. The average monsoon-season rainfall in this region is about 1000 mm. Therefore the interpretation of the additional 200 mm or 1.2 times more rainfall compared with past events including 1995 and 2006 can greatly affect the understanding of the 2011 flood hazard characteristic.

Oldenborgh et al. (2012) analyzed a long-term rainfall pattern in the region with the Global Precipitation Climatology Center (GPCC) V5 product. Based on the analysis,

NHESSD
2, 7027–7059, 2014

they concluded that the 2011 monsoon rainfall was not very unusual from a viewpoint of large-scale meteorology. They pointed out that the main causes of the unprecedented flood damage lay in the conversion of agricultural land into industrial complexes due to high vulnerability to flooding. Komori et al. (2012) highlighted the seemingly insignificant rainfall may contribute significantly to increase in runoff volume in the Chao Phraya River basin. They conceptually explained that the 1.4 times rainfall of normal years might result in 2.5 times more runoff of normal years under a constant evapotranspiration assumption. Kotsuki and Tanaka (2013) performed hydrologic simulation with a land surface model and concluded also that runoff is highly sensitive to rainfall (2.25 times more than average) in a naturalized condition excluding dam effects.

These studies are in line of hydrologic sensitivity analyses. Schaake (1990) introduced an elasticity index to quantify the runoff change to precipitation change as Eq. (1).

$$\varepsilon_Q = \frac{\mathrm{d}Q/Q}{\mathrm{d}P/P} = \frac{\mathrm{d}Q}{\mathrm{d}P}\frac{P}{Q} \tag{1}$$

The elasticity ε_Q represents how much runoff is expected to change, in percentage term, with a 1 % change in rainall. Schaake (1990) used a watershed hydrologic model with varying rainfall and temperature to estimate the elasticity of runoff. He found the elasticity is generally higher in drier conditions than wetter conditions. Dooge (1992) and Dooge et al. (1999) analytically derived the elasticity based on Budyko-type formula, and demonstrated the impact of seasonality and different climate conditions. Another approach is to use a regression model with historic records (Risbey and Entekhabi, 1996). Sankarasubramanian et al. (2001) summarizes the five types of approaches in hydrologic sensntivity studies. As the model based approach, Vano et al. (2012) used multiple land surface models, Mizukami et al. (2014) demonstrated the impact of different forcing data, and Vano et al. (2014) combined the sensitivity analysis with global circulation model output. One of the advantages for the model based approach is the ability to evaluate not only annual runoff but monthly or daily

NHESSD
2, 7027–7059, 2014

runoff variations. In fact, Shaake (1990) evaluated the monthly peak runoff to surrogate for the annual maximum flood in the elasiticiy estimation. However, to authors' best knwoledge, none of previous studies have estimated the elasticity of flood inundation, which is more directly related to the impact of floods in river basins with large delta areas (Dutta et al., 2003; Apel et al., 2006).

A possible reason for the luck of the inundation elasticity study may be associated to the difficulty in the flood inundation volume quantification, especially for the long term in large river basins. Most of existing inundation models are applied only to flood-plains and constrained by upstream river discharges. They are generally difficult to define if multiple locations are inundated in a large river basin. To take into account multiple inundations at various locations and their interactions in large river basins, this study employs a Rainfall-Runoff-Inundation (RRI) model (Sayama et al., 2012). The model simulates rainfall-runoff and flood inundation processes simultaneously on two-dimensional basis at a river basin scale. Since these two processes interact each other, the concept of the RRI model with rainfall forcing is thought to be suitable to estimate the elasticity of runoff and flood inundation.

The objective of this study is to quantify the sensitivity of flood runoff and inundation volumes to diagnose the characteristics of 2011 Thailand floods. We first calibrate the RRI model based on river discharge and tested the inundation simulation result with remote sensing as well as peak inundation water depths in 2011. Then we run the model continuously for 52 years (1960–2011) without the effect of dams and for 32 years (1980–2011) with the effect of two major dams. Based on the simulation results, we analyzed the relationship among rainfall, runoff and inundation volumes in different years including the 2011 for the entire Chao Phraya River basin. Finally we applied a regression model to the simulated historic runoff and inundation to estimate their elasticity indices.

NHESSD
2, 7027–7059, 2014

2 Method

This section explains the overview of the RRI model and its application to the Chao Phraya River basin, followed by the elasticity estimation method adopted in this study.

2.1 Structure of Rainfall-Runoff-Inundation model

The RRI model is a two-dimensional model capable of simulating rainfall-runoff and flood inundation simultaneously (Fig. 1) (Sayama et al., 2012). The model deals with land and river channels separately. In a grid cell where a river channel is located, the model assumes that both land and river are positioned within the same grid cell. The channel is discretized as a single line along its centerline of the overlying slope grid cell. The flow on the land grid cells is calculated with the 2-D diffusive wave model, while the channel flow is calculated with the 1-D diffusive wave model.

All the land grid cells can receive rainfall and contribute to rainfall-runoff flowing through other land grid cells and river channels. Meanwhile, they are subject to inundation due to multiple causes: overtopping from river channels, expansion of inundation water from surrounding land grid-cells, accumulation of local rainwater or any combination of the three. Hence, the RRI model does not structurally distinguish between rainfall-runoff and flood inundation processes; instead, it solves water flow hydrodynamically. In terms of its application to an entire river basin with rainfall input, the model is similar to grid cell-based distributed rainfall-runoff models. While typical rainfall-runoff models fix flow directions at each grid-cell based on surface topography, the RRI model change flow directions dynamically. In this regard, the RRI model is resemble to 2-D flood inundation models (e.g. Iwasa and Inoue; 1982). Nevertheless, unlike many other flood inundation models, the application of the RRI model is not limited to floodplains. It is applicable to an entire river basin. It simulates flow interactions between land and river channels with considerations of levees, so that the RRI model does not require specifying an overflowing point and its overtopping discharge, which are typically required as boundary conditions when using inundation models. Another

NHESSD
2, 7027–7059, 2014

feature of the RRI model is to accept rainfall and potential evapotranspiration as model input, and simulate surface and subsurface flow processes including flood inundation. The application of an integrated equation for surface and subsurface flows numerically solved by an adaptive time step Runge-Kutta algorithm (Cash and Karp, 1990; Press et al., 1992) enables the RRI model to run fast and stable calculation even for a large river basin with mountainous and plain areas.

2.2 Model application to the Chao Phraya River basin

The Chao Phraya River drains for the area of 160 000 km^2 from northern Thailand to the gulf of Thailand (Fig. 2). There are four major tributaries, i.e., Ping, Wang, Yom and Nan, flowing from the northern mountainous regions to the central point at Nakhon Sawan city. The upstream and downstream of Nakhon Sawan is a widespread lowland area, whose longitudinal gradient is approximately 1/12 000. The river section between Ayutthaya and Bangkok is even milder with a gradient of about 1/50 000. The bankfull discharges are about 3000–4000 $m^3 s^{-1}$ at Nakhon Sawan, about 2200–2900 $m^3 s^{-1}$ in the upstream and downstream of Ayutthaya (the main river is only about 1300 $m^3 s^{-1}$ at Ayutthaya after the diversion), and about 3600 $m^3 s^{-1}$ at Bangkok (Vongvisessomjai, 2007).

In the Chao Phraya River basin, there are two major dam reservoirs, the Bhumibol dam (13.5 billion m^3, in operation since 1964) located in the Ping River and the Sirikit dam (9.5 billion m^3, in operation since 1974) located in the Nan River. The primary purposes of the dam reservoirs are water resources and power generation. In 2011, the Bhumibol and Sirikit dam reservoirs were filled up to 45 and 51 % by 15 April, and then both were filled up to 95 % by 5 October and 14 September, respectively (Komori et al., 2013).

The RRI model is applied to the entire Chao Phraya River basin. As the model was being set up, DEM, flow direction and flow accumulation were delineated from HydroSHEDS 30 s (Lehner et al., 2008) and upscaled to 60 s (approximately 2 km) resolution (Masutani et al., 2006). Note that the RRI model uses flow direction and accumu-

NHESSD
2, 7027–7059, 2014

lation only to determine river channel locations but not for flood routing since the flow direction varies depending on local hydraulic gradients. River depths D [m] and widths W [m] were approximated first by Eqs. (2) and (3) (Coe et al., 2008), whose parameters were estimated from regression analysis with cross section data at 121 locations spreading over the entire basin.

$$W = C_W A^{S_W} \quad (2)$$

$$D = C_D A^{S_D} \quad (3)$$

where the obtained parameters were: $C_W = 16.93$, $S_W = 0.186$, $C_D = 2.48$, and $S_D = 0.12$. These equations capture the general characteristics of the river's cross-sections becoming wider and deeper toward the downstream. Nevertheless, the cross-sections need further improvement in some areas; for example, they cannot reproduce narrow sections well in the lower Yom River (Pakoksung et al., 2012, Sriariyawat et al., 2013). For particular cross-sections that the above empirical equations cannot represent well, we used cross-section data directly and replaced the values estimated by the equations.

The model input is rainfall and potential evapotranspiration. Daily rainfall records observed at about 400 stations were used after Thiessen polygon interpolation. Potential evapotranspiration was estimated with the Penman-Monthieth equation based on the European Centre for Medium-Range Weather Forecasts (ECMWF) reanalysis (Uppala et al., 2005). The Ecoclimap dataset (Tchuente et al., 2010), provided by Meteo France, was also used to identify seasonal and spatial variations of leaf area index.

To set model parameters, the area was first classified into two land cover areas: forest and cultivated area. The forest area is mainly distributed in upstream mountainous regions, where downslope subsurface flow and surface flow are simulated by taking both surface and subsurface flows into account (see detail in Sayama et al., 2012). On the other hand, the cultivated area including some urban areas is distributed mainly in downstream plain regions, where vertical infiltration and surface flow are simulated with the Green-Ampt equation.

NHESSD
2, 7027–7059, 2014

With respect to the effect of two major dams (Bhumibol and Sirikit), this study conducted two sets of simulation. The first one was a naturalized case, which did not take the dam effects into account, and used as the baseline simulation for water balance analysis. The simulation period for this case was 1960–2011 (52 years). The second case was to simulate water regulated conditions, which used reservoir outflow records as the boundary conditions at the two dam reservoirs. This regulated case was compared with the naturalized one to understand how the dams contributed to reduce flood runoff and inundation. The simulation period for the regulated case was limited to 1980–2011 (32 years) due to the availability of dam release records.

2.3 Water balance analysis

Based on the 52 year continuous rainfall-runoff-inundation simulation, we analyze basin-wide water balance for all the monsoon seasons. We calculate spatially averaged rainfall, actual evapotranspiration, runoff, catchment storage and flood inundation. The runoff in this study is defined as all the water volume flowing out from the river basin; i.e., discharge at the mouth of the Chao Phraya River basin as well as some flooded water flowing out directly from the basin into the sea. The catchment water storage is the total volumes of cumulative infiltrated volume within the G-A model, water height equivalent in soil and surface as well as water volume stored in the rivers. If surface water depths exceed 0.5 m due to accumulation of surface water, the volume of the water on land surface is considered as flood inundation volume and excluded from the catchment storage. Note that total volumes of simulated catchment storage and flood inundation are divided by area of the basin, so that all the water balance components have the same unit as average water depths in mm.

For the water balance analysis, the selection of period is very important. In this study, since our goal is to assess the relationship between rainfall and flood inundation volume, we first look at a period whose rainfall amount has the highest correlation with the maximum flood inundation volume. More specifically, by setting the maximum flood inundation date as the ending point of the water balance calculation period and changing

NHESSD
2, 7027–7059, 2014

the duration from one to seven months, we calculated correlation coefficients between rainfall amount during the selected period and the maximum flood inundation volume. For each simulation year, we calculate rainfall P, evapotranspiration ET, catchment storage change ΔS, total runoff Q, and flood inundation volume change ΔF in the selected period ending with each year's peak inundation arrival date. Note that ΔS and ΔF are used to describe the change in catchment storage and flood inundation volumes from the water balance point of view. However, since the flood inundation at the beginning of the rainy season is negligible, ΔF can be regarded as the peak flood inundation volume for each year. Based on the water balance, the following equation can be obtained:

$$P = \mathrm{ET} + Q + \Delta S + \Delta F \tag{4}$$

2.4 Elasticity index

The focus of this study is to understand the relationship between each term of the water balance equation including the flood inundation volume. We primarily focused on the $\mathrm{d}Q/\mathrm{d}P$ and $\mathrm{d}\Delta F/\mathrm{d}P$ to estimate how much runoff and inundation volumes are expected to increase with increase in rainfall in absolute volume. In addition, to represent the sensitivities of runoff to rainfall variability, the elasticity index ε_Q (1) is also calculated (Schaake, 1990). Similarly the elasticity for flood inundation volume $\varepsilon_{\Delta F}$ can be defined as:

$$\varepsilon_{\Delta F} = \frac{d\Delta F/\Delta F}{dP/P} = \frac{d\Delta F}{dP}\frac{P}{\Delta F} \tag{5}$$

Note that the indices contain the term of $\mathrm{d}\Delta F/\mathrm{d}P$ and quantify how much inundation volumes is expected to increase, in percentage term, with a 1 % increase in rainfall.

NHESSD
2, 7027–7059, 2014

3 Model simulation results

3.1 River discharge

Figure 3 shows simulated and observed monthly discharge at Nakhon Sawan (C2). We split the period between 1980 and 2011 into a calibration period (1980–1999) and a validation period (2000–2011). Model parmeters were then manually calibrated by focusing on the naturalized C2 monthly discharge. The naturalized discharge is estimated to avoid the effect of dams by adding inflow and subtracting outflow from the two major dam reservoirs to the observed monthly discharge. Note that the following sensitivity analysis covers the period of 1960–2011. However, due to the reliability of observed discharges, we focused here only on 1980–2011 for the calibration and validation purposes. Two metrices including Nash and Sutcliffe Efficiency (NSE) is used to evaluate the model performance (see Appendix). The hydrograph in Fig. 3 shows that the model can reproduce C2 monthly river discharge faily well for both calibration (NSE = 0.89) and valiation (NSE = 0.89). For the other upstream locations, we evaluated the simulated monthly river discharge for the two periods (see Table 2). The performance of Y17 was comparatively poor, possibly due to the diversion channel located upstream of Y17 to the lower Nan River. Except for Y17, the range of NSE were 0.67 to 0.89 (average NSE = 0.81) in 1980–1999 and 0.74 to 0.92 (average NSE = 0.84). One of the possible reasons for the better score in the latter period may be associated to the accuracy of the data also.

3.2 Flood inundation

We test the RRI model performance also in terms of peak flood inundation extent. Figure 4 shows the simulated annual maximum flood inundation depths (upper panel) and remote sensing composites (lower panel). For 2011, we referenced information released by UNITAR's Operational Satellite Applications Programme (UNOSAT), which used multiple-satellite information for estimating the maximum flood extent in the 2011

NHESSD
2, 7027–7059, 2014

flood event in Thailand. For previous years when no UNOSAT information is available, we used composite images produced by the Geo-Informatics and Space Technology Development Agency (GISTDA) in Thailand.

For the 2011, Fig. 4 shows the reasonable agreement of peak flood inundation extent, especially in the downstream part of C2 point. For the upstream of C2, the simulation shows some underestimation; and as a result, the evaluation indices were 0.21 by Absolute Normalized Error (ANE) and 0.46 by goodness-of-fit (FIT). There are some possible causes for this underestimation. The remote sensing analysis may judge areas as flooded even with shallow depths of water standing in paddy fields; on the other hand, throughout this study, we used 0.5 m as a threshold for flood inundation. Furthermore, in the case of relatively shallow water flooding, water tends to be stagnant due to roads and paddy field ridges. However, the model cannot resolve micro-topography; as a result, water moves more smoothly in the model and may underestimate the flood inundation extent in fringed areas.

Except for the 2011, year 2006 and 2010 also experienced relatively wider inundation, compared with the other years. For these two years also, Fig. 4 shows some model underestimation similar to the case in 2011. For the other years, including 2005, 2007, 2008 and 2009, with relatively smaller inundation extents, the modeled areas agree with the extents based on the remote sensing images as shown in Fig. 4 and ANE statistics in Table 3. Simulating small flood areas from the continuous and basin-wide model is very difficult for various reasons including those mentioned in the previous paragraph. As a result, the FIT values of those years are smaller than that of the 2011 flood. Regardless of the uncertainties, the RRI model can reproduce well the inter-annual variability of flood inundation extents.

To assess the model performance of peak inundation levels, we also conducted a post-flood field survey in 2011. We used a high-spec GPS and handy laser telemeter to measure flood marks at 18 points along rivers and 23 points on the floodplauns. The average mean error and root mean square error were −0.1 and 0.7 m along the rivers, while they were 1.1 and 1.2 m on floodplains.

NHESSD
2, 7027–7059, 2014

4 Sensitivity of flood runoff and inundation

4.1 Water balance analysis based on long-term RRI simulation

After the model set up, we run the model for 52 years from 1960 to 2011. The simulation results are then analyzed to estimate all the water balance components described in Sect. 2.3. Figure 5 shows the result with the horizontal axis of the days of the year (DOY) from 1 January to 31 December. The vertical axes of the five panels show rainfall, actual evapotranspiration, runoff, catchment storage and flood inundation, respectively. The solid red-line shows the result of 2011, while the other gray thin lines show the ones from the remaining 51 years. The average values are shown in the solid black-lines.

Figure 5 shows the total volumes of rainfall, runoff and flood inundation in 2011 are generally much more than those in the other years. The trend of catchment water storage in 2011 was close to the average in January and February but it started to deviate from the average after the beginning of March. The estimated minimum and maximum catchment water storage in 2011 were about 500 and 1000 mm, respectively, while they were about 400 and 800 mm in the average year.

Figure 6 compares peak inundation volumes for each year and rainfall amount prior to the dates of the peak inundation volumes. Since the six month rainfall shows the highest correlation ($r = 0.85$) to the peak inundation volumes, hereafter we use the six months as the baseline period for the water balance analysis.

Figure 7 shows the relationship between six month rainfall P on the x axis and the other terms including ET, ΔS, Q and ΔF on the y axis for all the 52 years. The figure suggests that ET is almost constant irrespective of P, while the other terms tend to increase with the increase in P, except for ΔF in the range of P less than about 950 mm. The term ΔS also shows some correlation with P, although ΔS of 2011 suggests the possibility of plateauing with the increase of P.

NHESSD
2, 7027–7059, 2014

4.2 Elasticity of flood runoff and inundation volumes

The six month rainfall in 2011 was about 1400 mm; that was about 1200 mm in past large-scale floods and about 1000 mm in normal years as shown in Fig. 7. In case of 2011, the estimated ΔF was 157 mm, which means that 11 % of the total rainfall turns out to contribute to inundation ($\Delta F/P = 0.11$) if no dam reservoirs are taken into account. The figure also suggests that the slope of ΔF against P can be seen as nearly constant for the range of P greater than 950 mm. The estimated slope ($\mathrm{d}\Delta F/\mathrm{d}P$) by using a first order linear regression with top 35 year records ($P > 950$ mm) is 0.30 (Table 4). That means an additional 200 mm rainfall results in a 60 mm (= 200 mm × 0.30) increase in flood inundation volume. Hence the rainfall of 1400 mm in 2011 might have increased flood inundation volume by about 60 mm, compared with other previous large floods such as 1995 and 2006 under the naturalized condition.

Regarding the runoff component, we need careful interpretation of the figure. As we mentioned above, the ending point of the period for the water balance calculation was set to be at the peak of flood inundation for each year. However, for better understanding of runoff volume, it is necessary to extend the period to cover flood runoff even after its flood inundation peak. For this purpose, we extended the period for two months after its inundation peak and recalculated ΔF and Q. The results shown in Fig. 8a and b suggest that flood inundation becomes almost zero when the period is extended for additional two months. As a result, the runoff ratio (Q'/P') of 2011 becomes 0.27 and $\mathrm{d}Q'/\mathrm{d}P'$ was 0.54 (dash denote that the period is extended to eight months).

In the above discussions, we primarily focused on $\mathrm{d}Q/\mathrm{d}P$ and $\mathrm{d}\Delta F/\mathrm{d}P$ to estimate how much runoff and inundation volumes are expected to increase with increase in rainfall in absolute term. Using these estimated slopes of the regression lines, we can further calculate the elasticity indices defined in Eqs. (1) and (5) since they contain the term of $\mathrm{d}Q/\mathrm{d}P$ or $\mathrm{d}\Delta F/\mathrm{d}P$.

To understand the general characteristics of the index, we first take an example of a simple linear model of runoff $Q = aP + b$, where a and b are constants. The model

NHESSD
2, 7027–7059, 2014

suggests that even if dQ/dP is a constant (= a), elasticity ε_Q (= $aP/(aP+b)$) can be dependent on the reference P. For the robust estimation of elasticity, Sankarasubramanian et al. (2001) used a nonparametric estimator, in which a long-term mean of P is used as the reference. In the case of elasticity of flood inundation volume $\varepsilon_{\Delta F}$, however, long-term mean of P may not be suitable because flood inundation volume becomes nearly zero in a normal year; as a result, $\varepsilon_{\Delta F}$ approaches to infinity. Moreover, our interest here is in the sensitivity of flood inundation volume under flooding situations. Hence we use P = 1200 mm, representing six months rainfall in past large flood years, as references to estimate ε_Q and $\varepsilon_{\Delta F}$ based on the linear regression equations. The estimated $\varepsilon_Q$is 3.0, whereas the estimated $\varepsilon_{\Delta F}$ becomes 5.0, indicating that a 1 % increase in rainfall may cause more abrupt increases in flood inundation volume (+5.0 %) than runoff volume (+3.0 %) in this basin.

4.3 Effect of dam reservoirs

The above discussions assume naturalized conditions without consiering two major dam resoivoirs. Figure 8b and d shows the similar results as Fig. 8a and c but with consideration of the two main dam reservoirs. The result suggest that the two main dam reservoirs contributed to reduce ΔF by 26 mm (= 4.4 billion m^3) and also $d\Delta F/P$ from 11 to 9 %. Since the total capacity of the two dam reservoirs in 17 April 2011 (six months before the peak flood inundation), was 46 mm (= 7.5 billion m^3) and their storages were almost full when the flood inundation reached its peak in mid-October, the 26 mm out of 46 mm contributed to reduce the flood inundation volume and the rest of the volume was expected to reduce the river discharges. The estimated elasticity of runoff ε_Q is 2.3, while the estimated elasticity flood inundation volume $\varepsilon_{\Delta F}$ is 4.2, indicating that a 1 % increase in rainfall may cause more abrupt increases in flood inundation volume (+4.2 %) than runoff volume (+2.3 %) with the considerations of the two main dam reservoirs.

NHESSD
2, 7027–7059, 2014

4.4 Summary and limitations

Figure 9 summarizes the results of elasticity estimations that include effects of dam reservoirs. The figure compares three different magnitudes with different monsoon rainfall (i.e. 1000, 1200 and 1400 mm). The runoff in 2011 is estimated to be 329 mm, while its in average years is 132 mm. Therefore 1.4 times more rainfall resulted in 2.5 times more runoff compared to the average years. The ratio agrees with what has been reported by Komori et al. (2012) as 2.5 times and Kotsuki and Tanaka (2013) as 2.25 times.

The runoff elasticity (ε_Q) is estimated as 2.3 %. The elasticity is within the range of 1.0 to 2.5 generally estimated in the United States by Sankarasurbramanian et al. (2012). Relatively high runoff elasticity compared to the reported range in the United States may be related that moisture (precipitation) and energy (PET) are "out of phase" of the monsoon climate in Thailand. The seasonality also causes ε_Q high in addition to dryness (Dooge et al., 1999).

The main focus of this study was to quantify flood inundation volume and its elasticity. The estimated elasticity for flood inundation (ε_F) was 4.2, which indicates that the inundation is more elastic than the runoff. The reasons of this high elasticity in the flood inundation are two folds. As Eq. (5) indicates, both $P/\Delta F$ and $\mathrm{d}\Delta F/\mathrm{d}P$ influence the elasticity. In general the first term tends to be large because flood inundation volume is much smaller compared with total rainfall; in case of 2011 this study estimated that the $P/\Delta F$ was 16.7 (= 1200 mm/72 mm). The second term ($\mathrm{d}F/\mathrm{d}P$), which is more important for sensitivity in absolute volumes, our analysis in Fig. 7 showed that the slope of the regression line was 0.25. This means that additional 200 mm rainfall increases 50 mm of flood inundation. If we convert this 50 mm to inundation volume by multiplying the area of the river basin, it turns out 8.0 billion m^3. The value is equivalent more than 80 % of the second largest dam namely the Sirikit dam reservoir (9.8 billion m^3). Multiplication of the two terms ($P/\Delta F$ and $\mathrm{d}\Delta F/\mathrm{d}P$) resulted in the high elasticity (ε_F = 4.2) of the flood inundation volume.

NHESSD
2, 7027–7059, 2014

The elasticity estimation approach presented in this study is the combination of model simulation based and historic regression based approaches. The advantage of this approach is to avoid assuming artificial spatial and temporal rainfall patterns typically necessary for the synthetic model based approach. Instead of using historic records of flood inundation, whose direct observation does not exist, we used the RRI model to estimate historic flood runoff and inundation volumes. Errors in the simulation can be the main source of the uncertainty in the estimations. Furthermore the deviations from the regression line shown in Fig. 7 can be another source of the uncertainty. To reduce the second uncertainty, it is necessary to match the temporal scale of target rainfall suitable for management objectives. This study choose six month rainfall prior to the peak of flood inundation as the basis for the analysis. The remaining deviations from the regression line in Fig. 7 indicate the flooding cannot be simply quantified only with six month rainfall; instead other factors including spatial and temporal rainfall patterns, antecedent conditions and many other factors influence the flooding. Therefore we need a hydrologic-hydrodynamic simulation model to estimate the flooding in detail. Regardless the uncertainty, our target of this study is to provide the first-order estimates of water balance components and their elasticity, which helps to quantitatively understand the nature of flood hazard in this region.

5 Conclusions

This study estimated the elasticity of flood runoff and inundation in the Chao Phraya River basin. Due to the flat topography with comparatively small bankfull river drainage, the delta suffers from frequent flood inundations. In this kind of environment, estimations of flood runoff and inundation and their sensitivites are essential for better flood risk management. The objective of this study is to quantify the sensitivity of flood runoff and inundation to address why the 2011 Thailand flood became so catastrophic with 1.2 times more or additional 200 mm more rainfall than past large floods including the ones in 1995 and 2006.

NHESSD
2, 7027–7059, 2014

Our analysis suggested that inundation volumes in this basin have the highest correlation with rainfall amount in the previous six months. In the case of 2011, the basin received about 1400 mm of rainfall in the rainy season, and 9 % of the total rainfall flooded at the peak of inundation under the dam operations. The elasticity of flood inundation volume to rainfall ε_Q was estimated as 4.2 %, which is higher than that for runoff volume (2.3 %).

The analysis shows two important implications in flood management. The first one is on diagnostic analysis of flood events. In the case of the 2011 flood, dam operations and other diversion channel management were claimed as primary causes of the devastating disaster. Seemingly small rainfall variability (i.e. 200 mm in six months) compared to past experienced flood events in the region tends to draw less attention to the magnitude of the event itself. However, our analysis suggested that the flood inundation volume was about 1.6 times (= 329 mm/213 mm) more than past events. Ignoring the amount misinterprets the dominant cause of flooding and thus may misguides future management policy. It is inevitable to quantify water balance by calculating from rainfall to runoff and inundation in diagnostic analysis of flood disasters.

The second implication is in climate change impact assessment. The analysis indicated the high sensitivity of flood inundation volume to rainfall variability in this basin. This provides an important perspective in terms of climate change vulnerability to flooding. Although a further study is necessary for issues related to climate change including temperature and other meteorological condition changes, the presented $\mathrm{d}\Delta F/\mathrm{d}P$ value, together with $\mathrm{d}Q/\mathrm{d}P$, should be useful indicators for characterizing how climate change may impact flooding in particular basins. Finally the presented rainfall–runoff-inundation simulation at large river basin scale should be an effective approach for the analysis of flooding including the assessment of climate change.

NHESSD
2, 7027–7059, 2014

Appendix A: Performance measures used in this study

To evaluate the model performance with respect to simulated discharge against observed discharge, we used Nash and Sutcliffe Model Efficiency (NSE):

$$\mathrm{NSE} = 1 - \frac{\sum (Q_{\mathrm{sim}}(t) - Q_{\mathrm{obs}}(t))^2}{\sum \left(Q_{\mathrm{obs}}(t) - \overline{Q_{\mathrm{obs}}}\right)^2} \tag{A1}$$

where $Q_{\mathrm{sim}}(t)$ and $Q_{\mathrm{obs}}(t)$ are simulated and observed discharge at timestep t and $\overline{Q_{\mathrm{obs}}}$ is average observed discharge in time. NSE is a composite measure of bias and random errors and the value becomes 1 for perfect prediction and 0 if prediction is no better than the average, and negative for worse than the average.

To evaluate the model performance for flood inundation extents, we used two indices including a goodness-of-fit (FIT) and the Absolute Normalized Error (ANE) of flood inundation area and defined as follows:

$$\mathrm{FIT} = \frac{\mathrm{IA}_{\mathrm{obs}} \cap \mathrm{IA}_{\mathrm{sim}}}{\mathrm{IA}_{\mathrm{obs}} \cup \mathrm{IA}_{\mathrm{sim}}} \tag{A2}$$

$$\mathrm{ANE} = \left| \frac{A_{\mathrm{sim}} - A_{\mathrm{obs}}}{A_{\mathrm{obs}}} \right| \tag{A3}$$

where $\mathrm{IA}_{\mathrm{sim}}$ and $\mathrm{IA}_{\mathrm{osb}}$ are flood inundation extents estimated by the simulation and remote sensing, while A_{sim} and A_{obs} are the areas of flood inundation extents estimated by the simulation and remote sensing. If both estimations overlap the area perfectly, FIT becomes 1 and ANE becomes 0. If the area of flooding are the same by simulation and remote sensing but the two extent do not overlap at all, then both FIT and ANE become zero.

Acknowledgements. The authors would like to express deep gratitude to Royal Irrigation Department (RID) and Thai Meteorological Department (TMD) for providing us observed records.

NHESSD
2, 7027–7059, 2014

The discussions with the JICA project team on a Comprehensive Flood Management Plan for the Chao Phraya River Basin, Anurak Sriariyawat at Chulalongkorn University in Thailand, Daisuke Komori at Tohoku University and Taichi Tebakari at Toyama Prefectural University help us understand the 2011 flood hazard in Thailand. The authors would like to thank Susumu Fujioka, Tomoki Ushiyama, Atsuhiro Yorozuya, Kuniyoshi Takeuchi at ICHARM for their support during the post-flood data correction and analysis. This research was funded by MEXT KAKENHI (Grant-in-Aid for Scientific Research (C), 24560633) and Grants supported by the Public Works Research Institute of Japan.

References

Apel, H., Thieken, A. H., Merz, B., and Bloschl, G.: A probabilistic modelling system for assessing flood risks, Nat. Hazards, 38, 79–100, doi:10.1007/s11069-005-8603-7, 2006.

Cash, J. R. and Karp, A. H.: A variable order Runge-Kutta method for initial value problems with rapidly varying right-hand sides, ACM T. Math. Software, 16, 201–222, 1990.

Coe, M. T., Costa, M. H., and Howard, E. A.: Simulating the surface waters of the Amazon River basin: impacts of new river geomorphic and flow parameterizations, Hydrol. Process., 22, 2542–2553, doi:10.1002/hyp.6850, 2008.

Dooge, J. C. I.: Sensitivity of runoff to climate change: a Hortonian approach, B. Am. Meteorol. Soc., 73, 2013–2024, 1992.

Dooge, J. C. L., Bruen, M., and Parmentier, B.: A simple model for estimating the sensitivity of runoff to long-term changes in precipitation without a change in vegetation, Adv. Water Resour., 23, 153–163, doi:10.1016/S0309-1708(99)00019-6, 1999.

Dutta, D., Herath, S., and Musiake, K.: A mathematical model for flood loss estimation, J. Hydrol., 227, 24–49, doi:10.1016/S0022-1694(03)00084-2, 2003.

Iwasa, Y. and Inoue, K.: Mathematical simulation of channel and overland flood flows in view of flood disaster engineering, J. Nat. Disaster Sci., 4, 1–30, 1982.

Kotsuki, S. and Tanaka, K.: Impacts of mid-rainy season rainfall on runoff into the Chao Phraya River, Thailand, J. Disaster Res., 8, 397–405, 2013.

Komori, D., Nakamura, S., Kiguchi, M., Nishijima, A., Yamazaki, D., Suzuki, S., Kawasaki, A., Oki, K., and Oki, T.: Characteristics of the 2011 Chao Phraya River flood in central Thailand, Hydrol. Res. Lett., 6, 41–46, doi:10.3178/HRL.6.41, 2012.

NHESSD
2, 7027–7059, 2014

Komori, D., Mateo, C. M., Saya, A., Nakamura, S., Kiguchi, M., Klinkhachorn, P., Sukhapunnaphan, T., Champathong, A., Takeya, K., and Oki, T.: Application of the probability evaluation for the seasonal reservoir operation on flood mitigation and water supply in the Chao Phraya River watershed, Thailand, J. Disaster Res., 8, 432–446, 2013.

Lehner, B., Verdin, K., and Jarvis, A.: New global hydrography derived from spaceborne elevation data, Eos Trans. AGU, 89, 93–94, 2008.

Masutani, K., Akai, K., and Magome, J.: A new scaling algorithm of gridded river networks, J. Japan Soc. Hydrol. Water Resour., 19, 139–150, 2006 (in Japanese with English abstract).

Mizukami, N., Clark, M. P., Slater, A. G., Brekke, L. D., Elsner, M. M., Arnold, J. R., and Gangopadhyay, S.: Hydrologic implications of different large-scale meteorological model forcing datasets in mountainous regions, J. Hydrometeorol., 15, 474–488, doi:10.1175/JHM-D-13-036.1, 2014.

Oldenborgh, G. J. V., Urk, A. V., and Allen, M. R.: The absence of a role of climate change in the 2011 Thailand floods, B. Am. Meteorol. Soc., 93, 1047–1049, doi:10.1175/BAMS-D-12-00021.1, 2012.

Pakoksung, K., Koontanakulvong, S., and Sriaiyawat, A.: Satellite data application for flood simulation, Proc. of PAWEES 2012 International Conference, 27–29 November 2012, Thailand, 2012.

Press, W. H., Teukolsky, S. A., Vetterling, W. T., and Flannery, B. P.: Adaptive stepsize control for Runge-Kutta, Numerical Recipes in Fortran 77: The Art of Scientific Computing, 2nd Edition, Cambridge University Press, New York, USA, 708–716, 1992.

Sankarasubramanian, A., Vogel, R. M., and Limbrunner, J. F.: Climate elasticity of streamflow in the United States, Water Resour. Res., 37, 1771–1781, doi:10.1029/2000WR900330, 2001.

Sayama, T., Ozawa, G., Kawakami, T., Nabesaka, S., and Fukami, K.: Rainfall-runoff-inundation analysis of the 2010 Pakistan flood in the Kabul River basin, Hydrol. Sci. J., 57, 298–312, doi:10.1080/02626667.2011.644245, 2012.

Schaake, J. C.: From climate to flow, in: Climate Change and US Water Resources, edited by: Waggoner, P. E., John Wiley, New York, 177–206, 1990.

Sriariyawat, A., Pakoksung, K., Sayama, T., Tanaka, S., and Koontanakulvong, S.: Approach to estimate the flood damage in Sukhothai Province using flood simulation, J. Disaster Res., 8, 406–414, 2013.

Tchuente, A. M. T., Roujean, J. L., and Faroux, S.: ECOCLIMAP-II: An ecosystem classification and land surface parameters database of Western Africa at 1 km resolution for the African

NHESSD
2, 7027–7059, 2014

Monsoon Multidisciplinary Analysis (AMMA) project, Remote Sens. Environ., 114, 961–976, doi:10.1016/j.rse.2009.12.008, 2010.

The World Bank: Thai Flood 2011, Rapid Assessment for Resilient Recovery and Reconstruction Planning, World Bank, Bangkok, 2012.

Uppala, S. M., Kållberg, P. W., Simmons, A. J., Andrae, U., Bechtold, V. D. C., Fiorino, M., Gibson, J. K., Haseler, J., Hernandez, A., Kelly, G. A., Li, X., Onogi, K., Saarinen, S., Sokka, N., Allan, R. P., Andersson, E., Arpe, K., Balmaseda, M. A., Beljaars, A. C. M., Berg, L. V. D., Bidlot, J., Bormann, N., Caires, S., Chevallier, F., Dethof, A., Dragosavac, M., Fisher, M., Fuentes, M., Hagemann, S., Hólm, E., Hoskins, B. J., Isaksen, L., Janssen, P. A. E. M., Jenne, R., Mcnally, A. P., Mahfouf, J.-F., Morcrette, J.-J., Rayner, N. A., Saunders, R. W., Simon, P., Sterl, A., Trenberth, K. E., Untch, A., Vasiljevic, D., Viterbo, P. and Woollen, J.: The ERA-40 re-analysis, Q. J. Roy. Meteor. Soc., 131, 2961–3012, doi:10.1256/qj.04.176, 2005.

Vano, J. A., Das, T., and Lettenmaier, D. P.: Hydrologic sensitivities of Colorado River runoff to changes in precipitation and temperature, J. Hydrometeorol., 13, 932–949, doi:10.1175/JHM-D-11-069.1, 2012.

Vano, J. A. and Lettenmaier, D. P.: A sensitivity-based approach to evaluating future changes in Colorado River discharge, Climatic Change, 122, 621–634, doi:10.1007/s10584-013-1023-x, 2014.

Vongvisessomjai, S.: Flood mitigation master plan for Chao Phraya Delta, 4 INWEPF Steering Meeting and Symposium, Bangkok, Thailand, 5–7 July 2007, 1–04, 2007.

NHESSD
2, 7027–7059, 2014

Table 1. Model parameter setting. The entire river basin is categorized into two regions: mountain and plain areas. Type S-S (surface + subsurface) with Eq. (4) is applied to the mountain area, while Type S-I (surface + infiltration) with Eq. (2) is applied to the plain area. The G-A model parameters are referred to (Raws et al., 1992). F_{limit} is an upper limit for the cumulative infiltration depth F in the G-A model. n_{river} is the Manning's roughness for river channels.

Parameters	Mountains	Plains
n [$\text{m}^{-1/3}\,\text{s}$]	0.35	0.35
d_a [m]	3.0	–
d_m [m]	1.5	
k_a [$\text{m}\,\text{s}^{-1}$]	0.01	–
β [–]	8.0	–
k_v [$\text{cm}\,\text{h}^{-1}$]	–	0.06
φ	–	0.471
S_f	–	0.273
F_{limit} [m]	–	0.4
n_{river} [$\text{m}^{-1/3}\,\text{s}$]	0.03	

NHESSD
2, 7027–7059, 2014

Table 2. Model performance evaluated by Nash-Sutcliffe Efficiency (NSE) for river discharges at gauging locations and two dam sites (B. Dam: Bhumibol Dam, S. Dam: Sirikit Dam). Parameters are calibrated for the discharge at C2 location between 1980 and 1999.

	Calibration (1980–1999)	Validation (2000–2011)
C2	0.89	0.89
N1	0.87	0.92
P1	0.67	0.79
Y1C	0.76	0.74
Y6	0.83	0.83
Y17	0.50	0.58
B. Dam	0.80	0.79
S. Dam	0.87	0.91

NHESSD
2, 7027–7059, 2014

Table 3. Model performance for flood inundation extent. ANE is absolute normalized error of flood inundation areas between simulations and remotely sensing. FIT is goodness-of-fit.

	ANE	FIT
2005	0.16	0.08
2006	0.47	0.31
2007	0.18	0.14
2008	0.05	0.15
2009	0.01	0.12
2010	0.52	0.25
2011	0.21	0.46
Avg.	0.23	0.21

NHESSD
2, 7027–7059, 2014

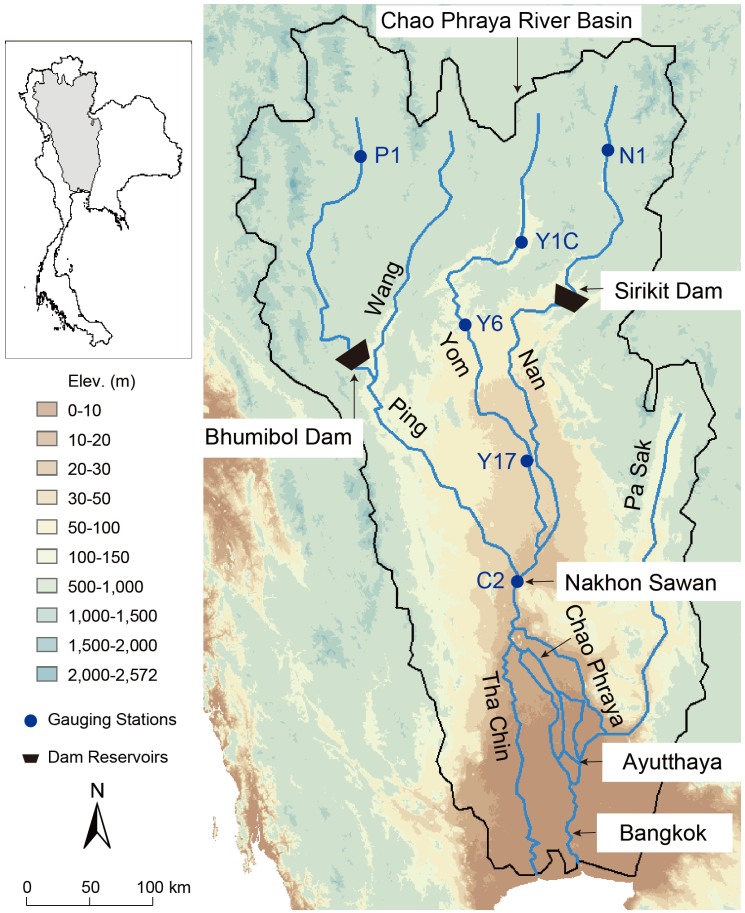

Figure 1. Map of the Chao Phraya River basin.

NHESSD
2, 7027–7059, 2014

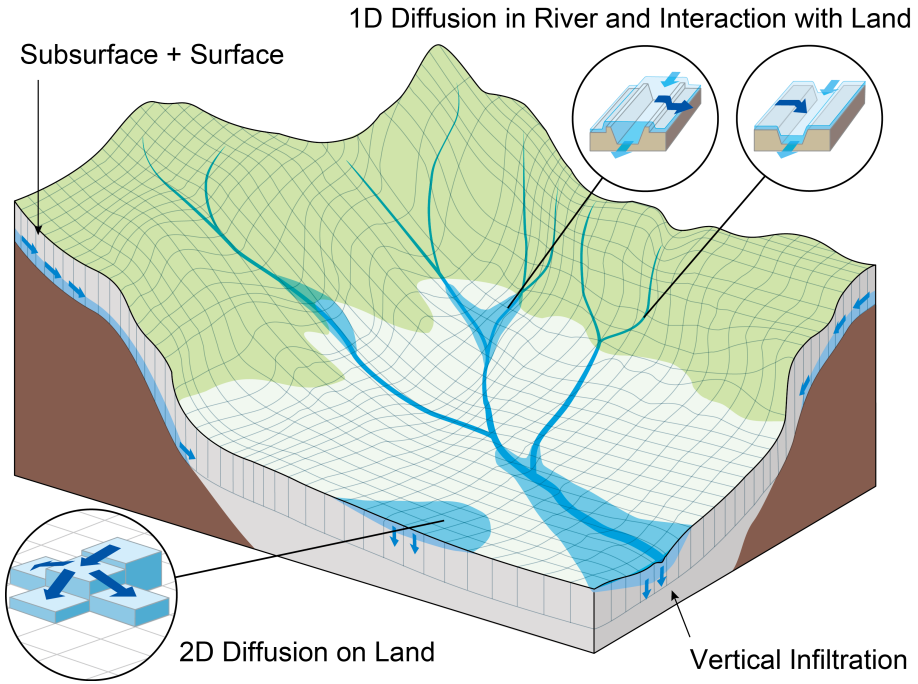

Figure 2. Schematic diagram of the RRI model.

NHESSD
2, 7027–7059, 2014

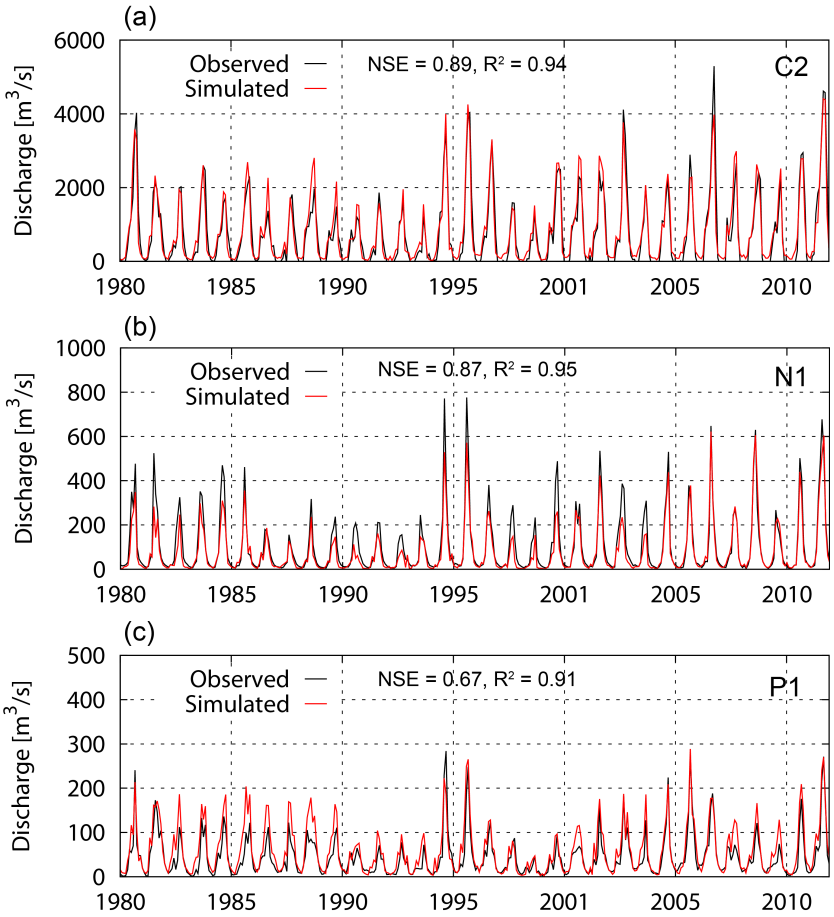

Figure 3. Simulated and observed monthly-averaged river discharges at **(a)** C2, **(b)** N1 and **(c)** P1.

NHESSD
2, 7027–7059, 2014

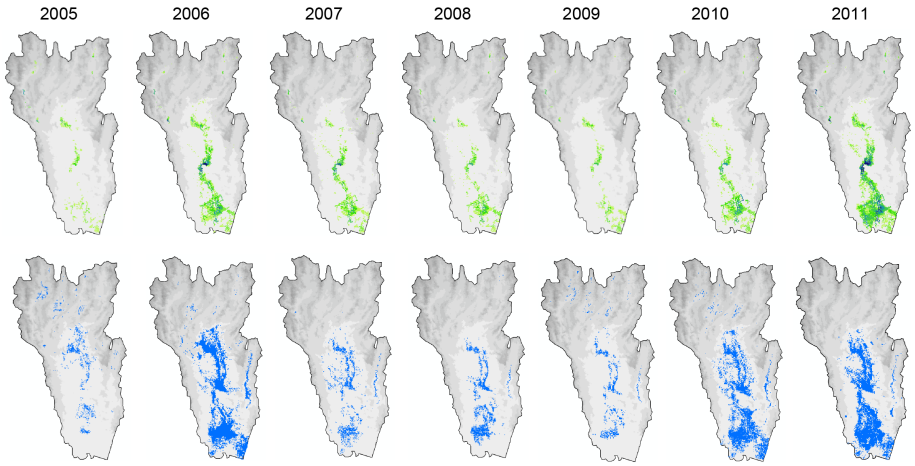

Figure 4. Simulated (upper panel) and remotely sensed (lower panel) annual maximum flood inundation extents from 2005 to 2011.

NHESSD
2, 7027–7059, 2014

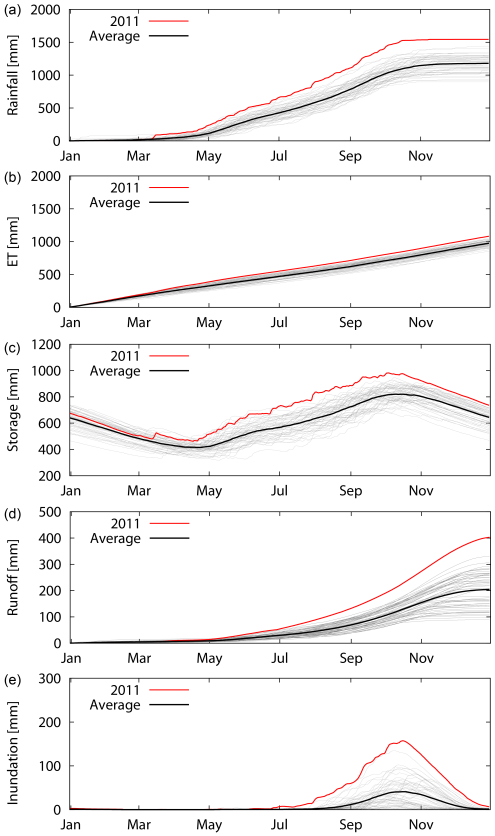

Figure 5. Simulated water balance components for 2011 (red lines), the other 51 years (gray lines) and average (gray lines): **(a)** cumulative rainfall, **(b)** evapotranspiration, **(c)** catchment storage volume, **(d)** runoff and **(e)** inundation volume.

NHESSD
2, 7027–7059, 2014

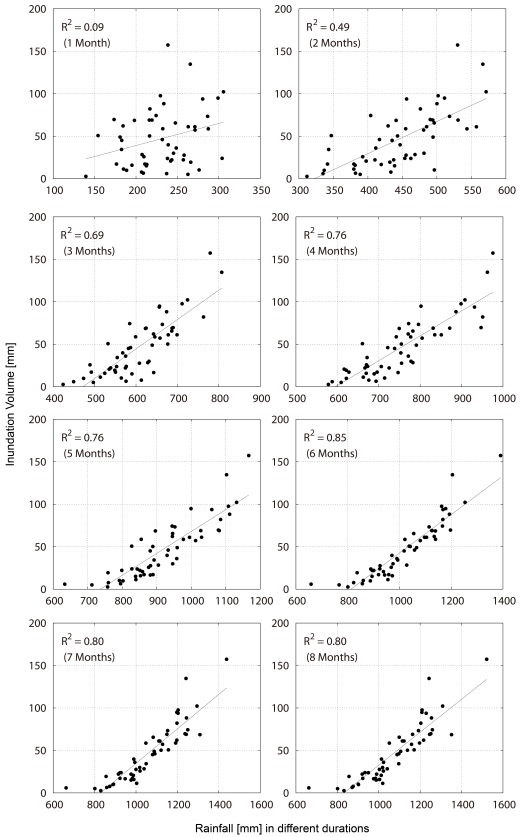

Figure 6. Relationships between annual maximum flood inundation volumes (*y* axis) and rainfall amount for different durations (*x* axis).

NHESSD
2, 7027–7059, 2014

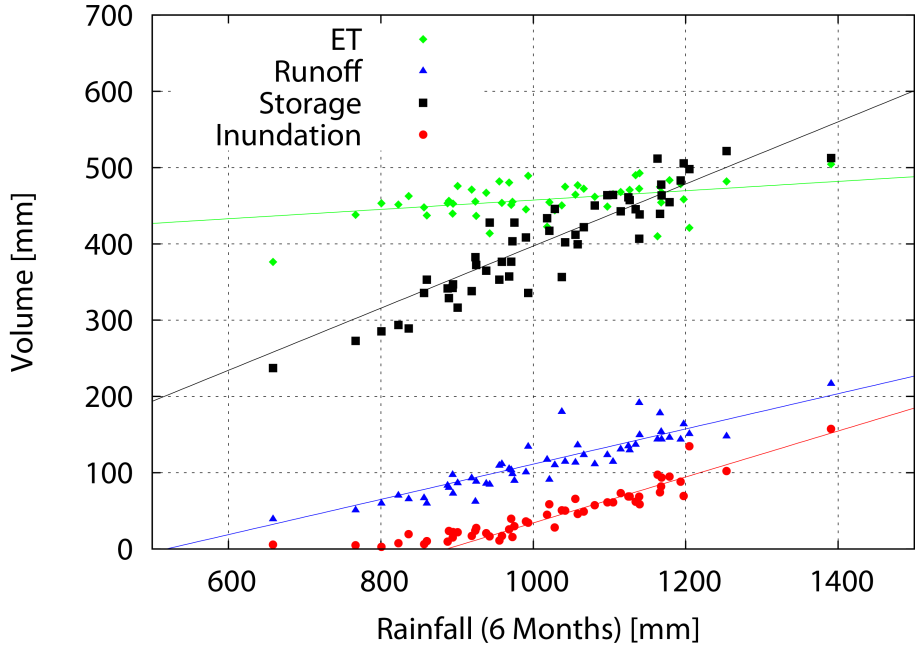

Figure 7. Relationship between precipitation (P) for six months and evapotranspiration (ET), total runoff (Q), storage change (ΔS) and inundation volume (ΔF). Dots show the results from different years based on the 52 year simulation (without dams).

NHESSD
2, 7027–7059, 2014

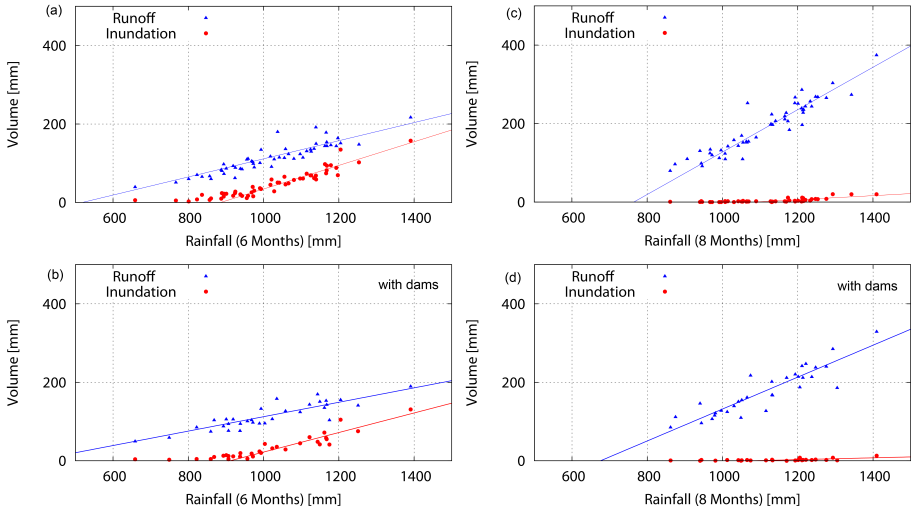

Figure 8. Relationship between precipitation (P) and discharge (Q) and inundation volume (ΔF). The panels **(a)** and **(c)** show the cases without dams, while **(b)** and **(d)** show the cases with dams. The difference between **(a)**, **(b)** and **(c)**, **(d)** are the period of the rainfall in the x axes. The x axes of **(a)** and **(b)** are the same as Fig. 7 (i.e. six month rainfall prior to the peaks of flood inundation volumes for each year), whereas the x axes of **(c)** and **(d)** are eight months rainfall (i.e. two more months are extended from the peaks of flood inundation volumes) to evaluate the relationship between rainfall amount and total runoff volumes.

NHESSD
2, 7027–7059, 2014

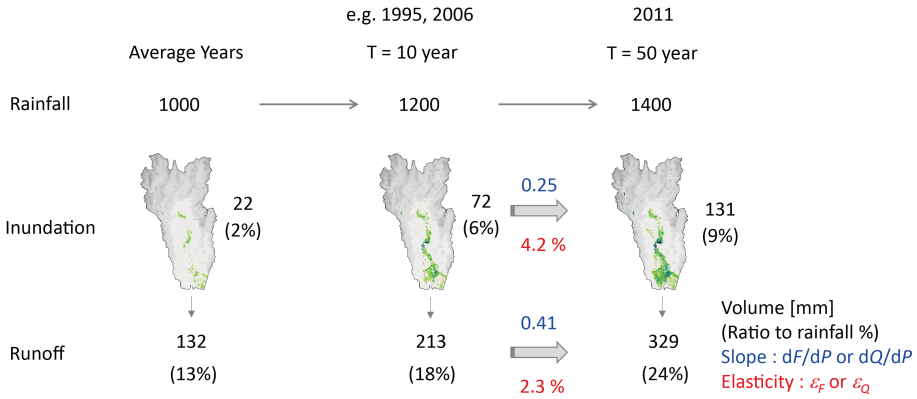

Figure 9. Summary sensitivity analysis on flood runoff and inundation volumes.

NHESSD
2, 7027–7059, 2014